International Journal of Mechanical, Industrial and Aerospace Sciences
ISSN: 2517-9950
Vol:10, No:2, 2016

A Computational Study on Flow Separation Control of Humpback Whale Inspired Sinusoidal Hydrofoils

J. Joy, T. H. New, I. H. Ibrahim

***Abstract*—**A computational study on bio-inspired NACA63$_4$-021 hydrofoils with leading-edge protuberances has been carried out to investigate their hydrodynamic flow control characteristics at a Reynolds number of 14,000 and different angles-of-attack. The numerical simulations were performed using ANSYS FLUENT and based on Reynolds-Averaged Navier-Stokes (RANS) solver mode incorporated with k-ω Shear Stress Transport (SST) turbulence model. The results obtained indicate varying flow phenomenon along the peaks and troughs over the span of the hydrofoils. Compared to the baseline hydrofoil with no leading-edge protuberances, the leading-edge modified hydrofoils tend to reduce flow separation extents along the peak regions. In contrast, there are increased flow separations in the trough regions of the hydrofoil with leading-edge protuberances. Interestingly, it was observed that dissimilar flow separation behaviour is produced along different peak- or trough-planes along the hydrofoil span, even though the troughs or peaks are physically similar at each interval for a particular hydrofoil. Significant interactions between adjacent flow structures produced by the leading-edge protuberances have also been observed. These flow interactions are believed to be responsible for the dissimilar flow separation behaviour along physically similar peak- or trough-planes.

***Keywords*—**Computational Fluid Dynamics, Flow separation control, Hydrofoils, Leading-edge protuberances.

I. Introduction

IN aerospace and marine engineering, drawing inspirations from nature has been the primary source of motivation for quite a number of engineering research [1]-[8] and applications. Recently, humpback whale pectoral flippers have gained significant attention because of their supposedly significant contribution towards the whales' good maneuvering capabilities. This is partially credited by the presence of the tubercles along the leading-edges of the whale pectoral flippers. The humpback whales are well-known for their breaching characteristics as well as ability to perform complex maneuvers underwater [1]. The morphology of humpback whale flippers and its swift behaviour at relatively lower Reynolds (Re) number has inspired various hydrofoil designs with leading edge protuberances over the past few years.

One of the first experimental analyses on an idealized whale flipper model was carried out in wind tunnel by [1] at Re=5×10^5. The findings indicate that it produced an increase in the maximum lift by 6% and delay in the stall angle-of-attack by 40%, as compared to a model without leading-edge protuberances. Performance analysis of swept wings with leading-edge protuberances at sweep angles 15° and 30° was carried out by [2]. Results indicate that the maximum lift values for the corresponding sweep angles were increased by 9% and 4% respectively. According to [4], however, there are significance differences in flow control characteristics of the modified aerofoils in pre- and post-stall conditions. It was reported that the performance of the modified aerofoils is inferior to the baseline hydrofoil in pre-stall conditions but vice versa in post-stall conditions [6]. Flow control analysis of hydrofoils with leading-edge protuberances was carried out by [8] at Re=1.4×10^4. The results indicate that the design of leading-edge protuberances deeply affect the flow control behaviour of the hydrofoils at a lower Reynolds number. Numerical investigations at Re=5×10^5 was also performed by [5] based on Detached-Eddy Simulation technique. The results indicate that the leading-edge protuberances are capable of reducing flow separations at the tip of the flippers at a higher Reynolds number.

In this paper, a computational investigation of the flow control characteristics and separation behaviour of a baseline (NACA 634-021) and two modified hydrofoils is carried out at Re=1.4×104 (Table I). The two modified hydrofoils, named 8L and 16L respectively, were designed such that they have the same wave amplitude but with the latter having half the former's wavelength, as shown in Fig. 1. The focus of this computational study is to look into the flow characteristics and comment upon the effects of protuberance wavelength, on top of looking at how close the flow simulation results are with respect to experiment results reported in the literature earlier. Furthermore, earlier investigations tend to be carried out at higher Reynolds numbers [1]-[3] than lower ones. Hence, this is a good opportunity to look into how these modified hydrofoils will perform at significantly lower Reynolds number flows.

II. Computational Approach

In the present study, a NACA 63$_4$-021 profiled hydrofoil is set as the reference hydrofoil, due to its close resemblance to the humpback whales pectoral flipper cross-section. A comparative study is carried out between this reference hydrofoil and two modified hydrofoils with leading-edge protuberances, namely 8L and 16L. The test models are similar to the ones used in the experimental study by Wei et al. [8] (Fig. 1), where the mean chord and span of all hydrofoils are c=75mm and b=300mm respectively. This led to hydrofoils with an aspect-ratio of b/c=4. The protuberance

J. Joy is with the Technische Universität München (ASIA), Singapore 139660 (e-mail: M130147@ntu.edu.sg).
T. H. New is with Nanyang Technological University, Singapore 639798 (corresponding author phone- +65-6790 4443; e-mail: dthnew@ntu.edu.sg).
I. H. Ibrahim is with the University of Glasgow, Singapore 599489 (e-mail: Imran.Ibrahim@glasgow.ac.uk).

wavelength for the 8L and 16L hydrofoils are λ=0.5c and λ=0.25c respectively, while a protuberance amplitude of A=0.12c is used for both the hydrofoils. The geometrical details of the three test hydrofoils are listed out in Table I.

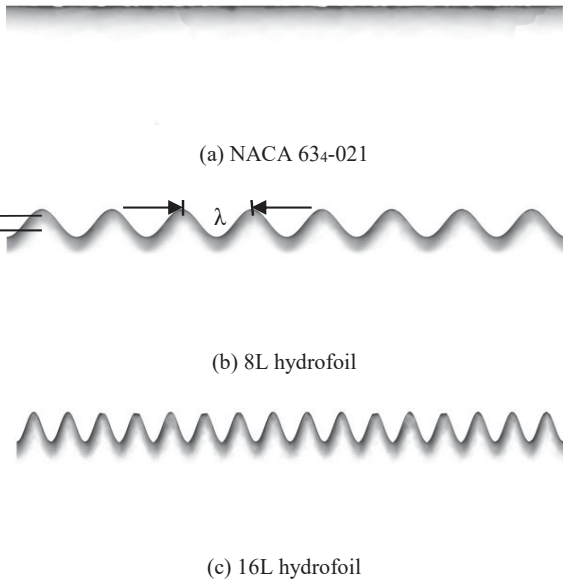

(a) NACA 63_4-021

(b) 8L hydrofoil

(c) 16L hydrofoil

Fig. 1 CAD designs of the three test hydrofoils

TABLE I
CONFIGURATION OF THE HYDROFOILS

Hydrofoil	λ (mm)	A (mm)
NACA 63_4-021	-	-
8L	37.5	9
16L	18.75	9

The computational investigation was carried out using ANSYS FLUENT. The domain size was defined to represent the water tunnel test section reported by [8]. The x- and y-coordinate dimensions of the computational domain were 500mm and 450mm respectively, while the z-coordinate dimension remains similar to the spans of the hydrofoils. Unstructured mesh technique (Fig. 2) was implemented on the domain with overall y^+ value of less than 5. The mesh was defined using the mesh sizing tools available in FLUENT. The simulations were carried out using k-ω Shear Stress Transport (SST) model with steady and unsteady Reynolds-Averaged Navier Stokes (RANS) governing equations. The single-precision transient model was applied for a time-duration of 10 seconds with a time step of 0.1. The results presented in the next section were taken from the final time step of the simulation. The flow inlet velocity is 0.19m/s with a turbulence intensity of 1.1%. The computational analysis was performed at the convergence criteria of 1×10^{-5}.

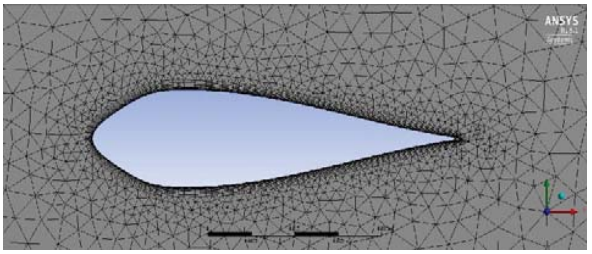

Fig. 2 A sample grid model of the 8L test hydrofoil

TABLE II
POSITION OF THE HYDROFOILS (X/B)

Hydrofoil	Trough-plane (x/b)	Mid-plane (x/b)	Peak-plane (x/b)
NACA 63_4-021	--	0.5	--
8L	0.5	--	0.56
	0.62		0.68
	0.75		0.81
	0.87		0.93
16L	0.5	0.51	0.53
	0.56	0.57	0.59
	0.62	0.64	0.65
	0.68	0.70	0.71
	0.75	0.76	0.78
	0.81	0.82	0.84
	0.87	0.89	0.90
	0.93	0.95	0.96

III. RESULTS AND DISCUSSION

Two-dimensional streamlines along the peak-, trough- and mid-planes were determined for all three test hydrofoils. The positions of these planes on the hydrofoil span are listed in Table II. For the baseline hydrofoil, the streamline patterns are visualized along the mid-span plane (i.e. x/b=0.5). For the 8L hydrofoil, streamline patterns at all the trough- and peak-planes are investigated, while for the 16L hydrofoil, streamline patterns at all the trough-, mid- and peak-planes are studied. As the present study will attempt to look at the overall flow separation behaviour along the entire hydrofoil span, these streamline patterns will be extracted and presented here.

Preliminary observations reveal that the computational results are in general agreements with the experimental results presented by [8]. For instance, the baseline hydrofoil shows flow separation behaviour associated with the relatively thick hydrofoil profile at low Reynolds numbers Fig. 3). At α=0°, the flow separation point lies around the half-chord of the reference hydrofoil and a flow separation bubble is formed at the rear end of the hydrofoil. As the angle-of-attack increases to α=10°, the flow separation point shifts upstream and closer to leading-edge. At α=15°, strong flow separation is observed and the flow separation bubble is quite prominent at this angle-of-attack. The streamline patterns are almost invariant along the span-wise direction of the reference.

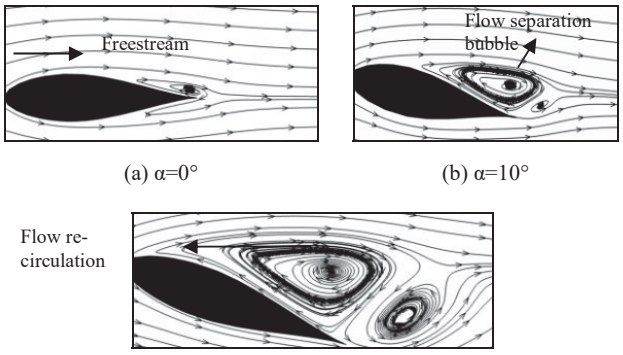

(a) α=0° (b) α=10°

(c) α=15°

Fig. 3 2D streamlines for the NACA63$_4$-021 reference hydrofoil at x/b=0.5 location

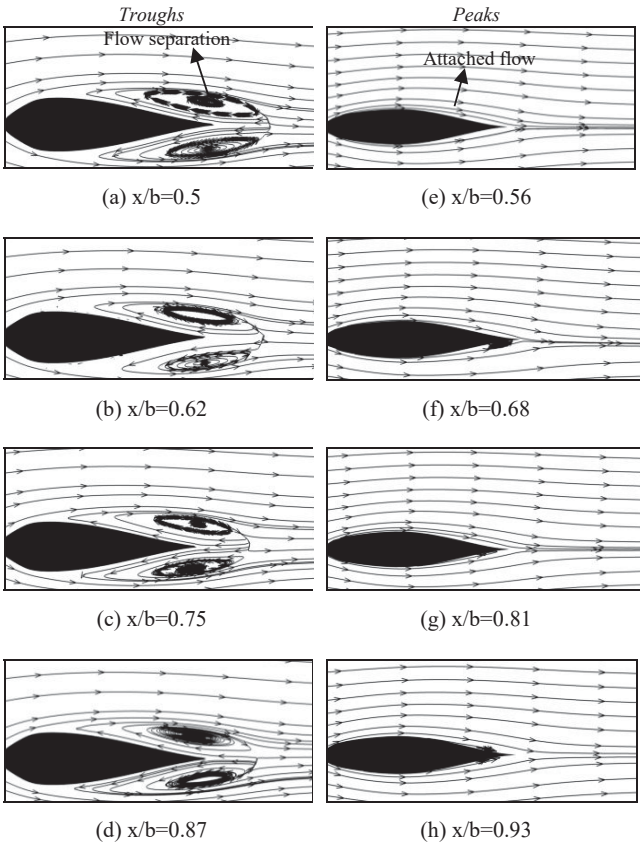

(a) x/b=0.5 (e) x/b=0.56

(b) x/b=0.62 (f) x/b=0.68

(c) x/b=0.75 (g) x/b=0.81

(d) x/b=0.87 (h) x/b=0.93

Fig. 4 Streamline patterns along various trough- and peak-planes for 8L hydrofoil at α=0°

Implementation of leading-edge protuberances in 8L and 16L test hydrofoils produces rather different flow characteristics along their span-wise directions. The first interesting observation is that the flow separation behaviour varies accordingly to the peak- and trough-planes of the hydrofoils with leading-edge protuberances, as will be demonstrated in the results to be presented. From these results, it will be seen that flow mitigation performance will generally be better along the peak-plane, rather than along the trough-plane, which again is in good agreement with the experimental results reported by [8]. Furthermore, it will be observed during the discussion later that the flow separation behaviour is sensitive towards the wavelength of the protuberances.

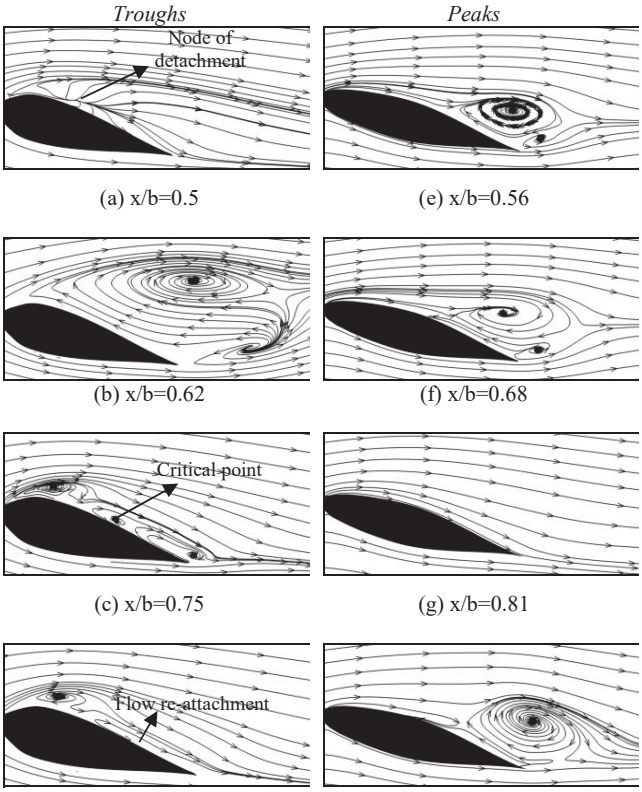

(a) x/b=0.5 (e) x/b=0.56

(b) x/b=0.62 (f) x/b=0.68

(c) x/b=0.75 (g) x/b=0.81

(d) x/b=0.87 (h) x/b=0.93

Fig. 5 Streamline patterns along various trough- and peak-planes for 8L hydrofoil at α=15°

For the 8L hydrofoil shown in Fig. 4, it is quite clear that mean flow separation behaviour along the upper and lower surfaces is very prominent along the trough-planes, even at α=0°. In contrast, very little mean flow separation can be observed along the peak-planes. The results also indicate that the mean flow separation behaviour at different trough- or peak-planes is very similar with one another. With such a significant discrepancy between the trough- and peak planes, strong presence of three-dimensional flows is expected to exist along the hydrofoil surfaces. At α=15° as shown in Fig. 5 however, flows along the trough-planes separates right at or very close to the leading-edges along the upper surfaces, which is in good agreement with the experimental results by [8]. The massive flow separation from the leading edge and re-circulation effects lead to the formation of laminar separation bubble along certain trough-planes. The most intriguing is that the streamline patterns appear to be very different between the different trough-planes, even though the troughs are geometrically similar. For instance, a strong re-circulating bubble can be observed at x/b=0.62 location while laminar separation bubbles can be seen at x/b=0.75 and 0.87 locations.

There exist large discrepancies in both the extent of the mean flow separation region, as well as behaviour. In fact, similar observations can also be made for the streamline patterns along the peak-planes at the same angle-of-attack. While most peak-planes demonstrate flow separations close to the mid-chord location to form significant flow separation bubbles along the trailing-edge region, one of them shows no discernible flow separation bubble at all. This has not been reported in the literature previously and one possible explanation is that the flow behaviour for hydrofoils modified with leading-edge protuberances, the flows are inherently highly unsteady at post-stall angles-of-attack.

Figs. 6-8 show the streamline patterns for the 16L hydrofoil at the trough-, mid- and peak planes at α=0° and 15°. Three-dimensional flow behaviour is much more obvious for this hydrofoil, probably due to the doubling of the leading-edge protuberances. The flow patterns in some trough regions (i.e. x/b=0.56, 0.62 and 0.68 locations) show massive flow separations, while the others (i.e. x/b=0.75, 0.81 and 0.87 locations) show little to no flow separations, the presence of critical points and laminar separation bubble. In particular, the presence of critical points indicates the presence of highly three-dimensional spanwise flows.

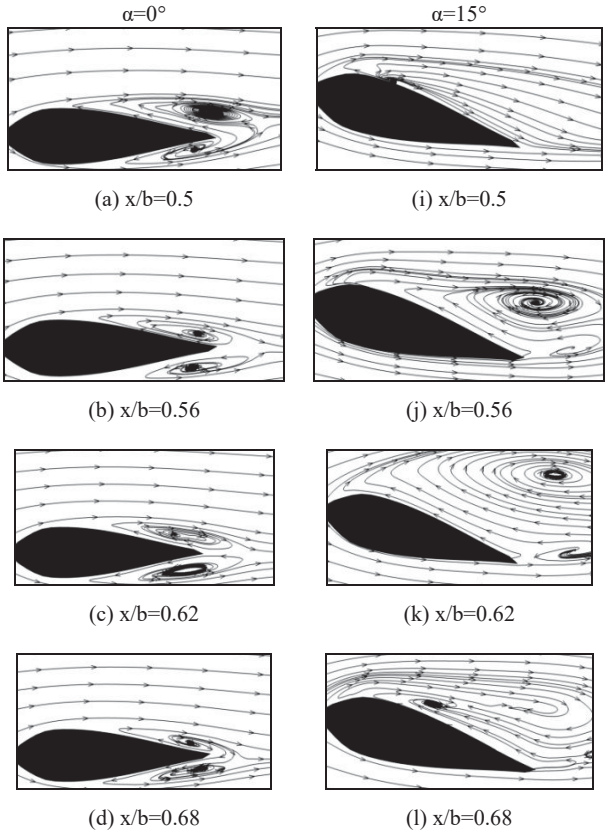

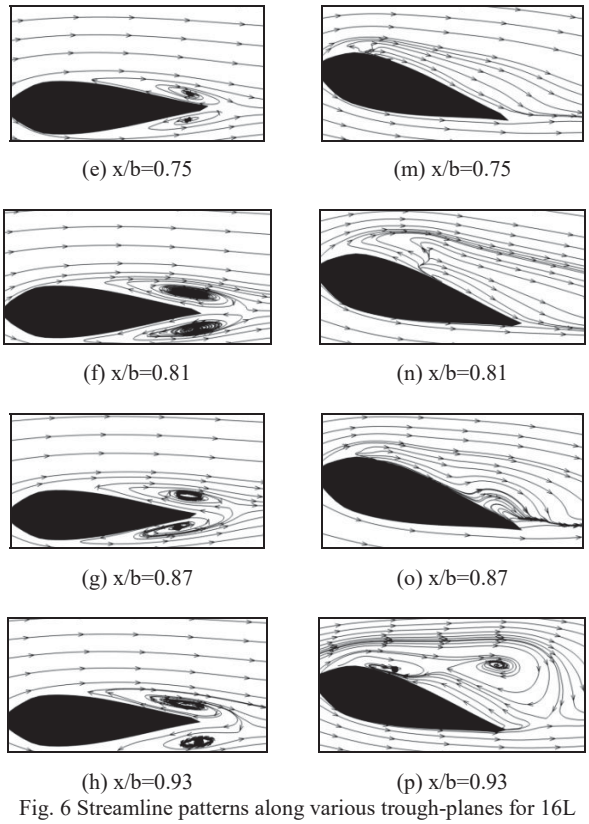

Fig. 6 Streamline patterns along various trough-planes for 16L hydrofoil at α=0° and 15°

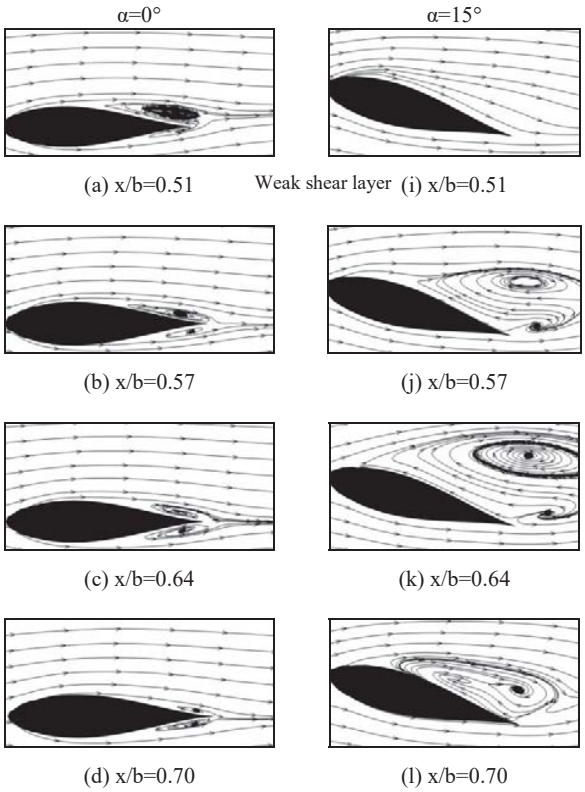

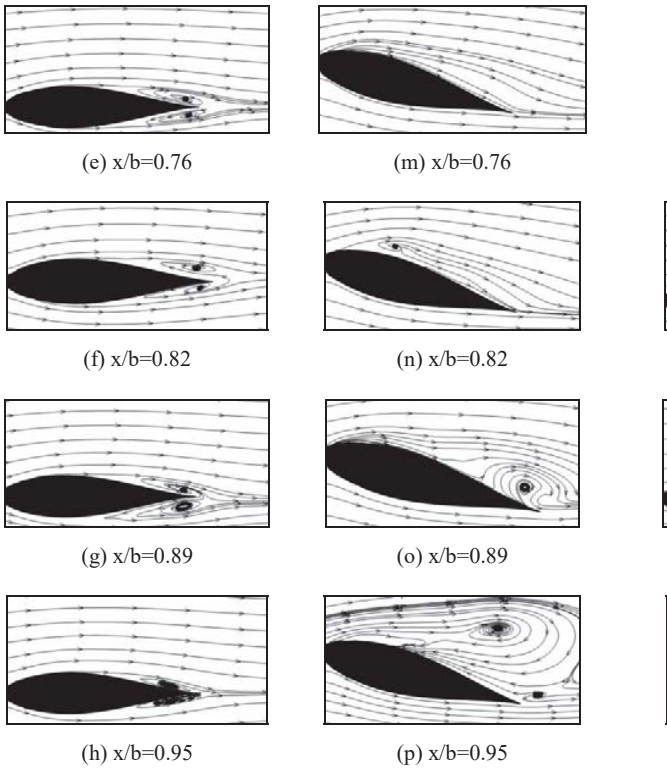

Fig. 7 Streamline patterns along various mid-planes for 16L hydrofoil at α=0° and 15°

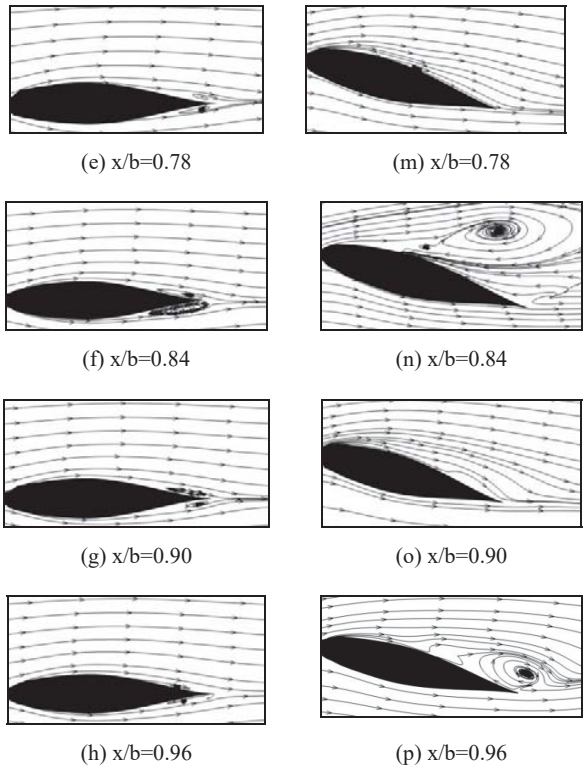

Fig. 8 Streamline patterns along various peak-planes for 16L hydrofoil at α=0° and 15°

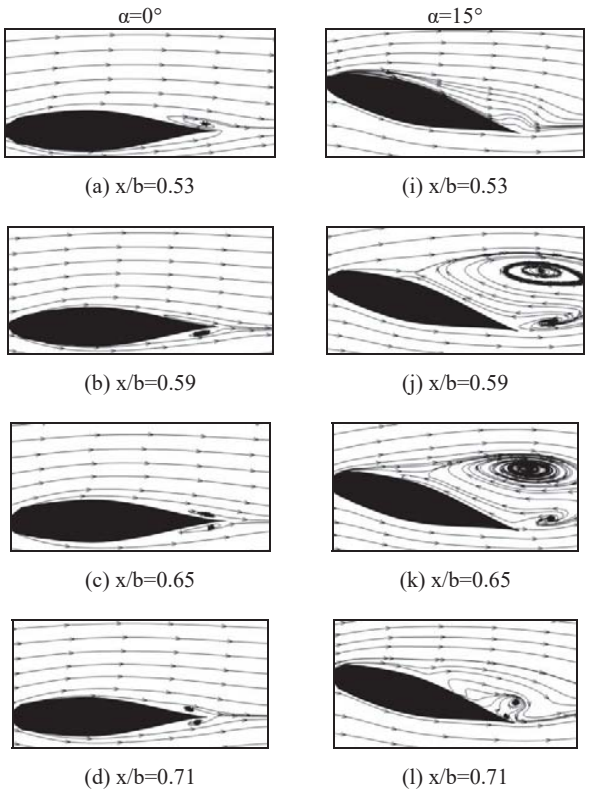

Fig. 9 Friction lines along 16L hydrofoil upper surface at α=0° and 15°

The wide range of different flow behaviour between different trough- or peak-plane is surprising. Hence, to investigate further, Figs. 9 and 10 show the wall friction lines on the upper surface, as well as the vorticity lines along the trailing-edge of the 16L hydrofoil at α=0° and 15°. In particular, Fig. 9 provides valuable clues as to why the flow separation behaviour appears to be so different between the different trough- or peak-planes. Closer inspection will reveal that, despite the regular appearance of flow features associated with the counter-rotating streamwise vortices, the flow paths along the upper hydrofoil surface are actually not that coherent, especially at α=15°. This may be indicative of the resulting flow behaviour if the incoming free-stream exceeds a certain turbulence level and manages to perturb the otherwise stable counter-rotating streamwise vortices sufficiently. Nevertheless, it remains possible that some currently unknown numerical issues have contributed towards the flow behaviour

observed in Fig. 9. Efforts are currently underway to investigate further on this.

Lastly, Fig. 10 shows that while the 16L hydrofoil produces regular counter-rotating streamwise vortices that leave their mark on the vorticity lines along the trailing-edge at α=0°, that is not quite the case at α=15°. Instead, two large vortical entities appear to have been formed along the trailing-edge. While the origin of these vortical entities remains unknown at this point, it is worthwhile to mention in passing here that a follow-up experimental study to [8] by the last author has produced some results that show grossly similar large-scale vertical behaviour.

(a) α=0°

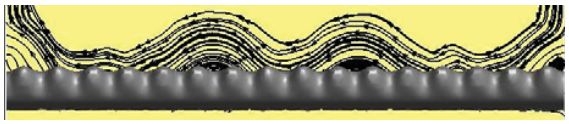

(b) α=15°

Fig. 10 Vorticity lines along 16L hydrofoil trailing-edge at α=0° and 15°

Conclusions

A preliminary computational study on a NACA63$_4$-021 reference hydrofoil and two hydrofoils with leading edge protuberances have been conducted at a Reynolds number of Re=1.4×10^4. Results show that flow separations occur earlier as compared to higher Reynolds number flow conditions. Generally speaking, the computational results obtained at α=0° and α=15° are in good agreement with the experimental results reported by [8] previously. More interestingly, detailed analysis of the streamline patterns along various trough-, mid- and peak-planes reveals that flow separation behaviour may differ even for geometrically similar troughs or peaks along a single hydrofoil modified with leading-edge protuberances. Surface flow lines suggest that strong three-dimensional effects are likely to be responsible, though efforts are currently underway to confirm this. Lastly, large-scale vortical entities along the trailing-edge of the 16L hydrofoil are observed, which have also been observed in another early experimental investigation by the last author.

Acknowledgments

The authors gratefully acknowledge the support provided for the study through a MINDEF Defense Innovative Research Project Research Grant, as well as assistance rendered by Z. Wei in designing the hydrofoils with leading-edge protuberances incorporated.

References

[1] Miklosovic, D.S., Murray M.M., Howie L.E., Fish F.E. Leading-edge tubercles delay stall on humpback whale (*Megaptera novaeangliae*) flippers, 2004. *Physics of Fluids.* 16 (5), 39-42.

[2] Murray, M.M., Fish, F.E., Howey, L.E., Miklosovic, D.S. Effects of leading edge tubercles on a representative whale flipper model at various sweep angles, 2005. In *Proceedings of the 14th International symposium on Unmanned Untethered Submersible Technology (UUST),* Autonomous undersea System Inst., Lee, NH.

[3] Johari, H., Henoch, C., Custodio, D., Levshin, A. Effects of leading-edge protuberances on airfoil performance, 2007. *AIAA Journal*. 45 (11), 2634-2643.

[4] Hansen, K.L., Kelso, R.M., Dally, B.B. Performance variations of leading-edge tubercles for distinct airfoil profiles, 2011. *AIAA Journal*. 49 (1), 185-194.

[5] Pedro H.T.C., Kobayashi M.H., Numerical study on stall delay on Humpback Whale flippers, 2008. *AIAA paper* number 2008-0584.

[6] Rostamzadeh N., Hansen K.L., Kelso R.M., Dally B.B., The effect of undulation leading-edge modifications on NACA 0021 airfoil characteristics, 2014, Physics of Fluids. 26, 107101.

[7] Zhang, M.M., Wang, G.F., Xu J.Z. Aerodynamic control of Low-Reynolds-Number airfoil with leading-edge protuberances, 2013. *AIAA Journal*. 51 (8), 1960-1971.

[8] Wei, Z., New, T.H., Cui, Y. An experimental study on flow separation control of hydrofoils with leading-edge tubercles at low Reynolds number, 2015. *Ocean Engineering*. 108, 336-349.